THE BASALTS OF MARE FRIGORIS. G. Y. Kramer[1†], B. Jaiswal[2], B. R. Hawke[3], T. A. Giguere[4], [1]Lunar and Planetary Insititute, Houston, TX, 77058, [2]ISRO Satellite Centre, Bangalore, Karnataka, India 560017, [3]Hawaii Institute of Geophysics and Planetology, University of Hawaii, Honolulu, HI 96822, [4]Intergraph Corporation, Kapolei, HI 96707, [†]kramer@lpi.usra.edu.

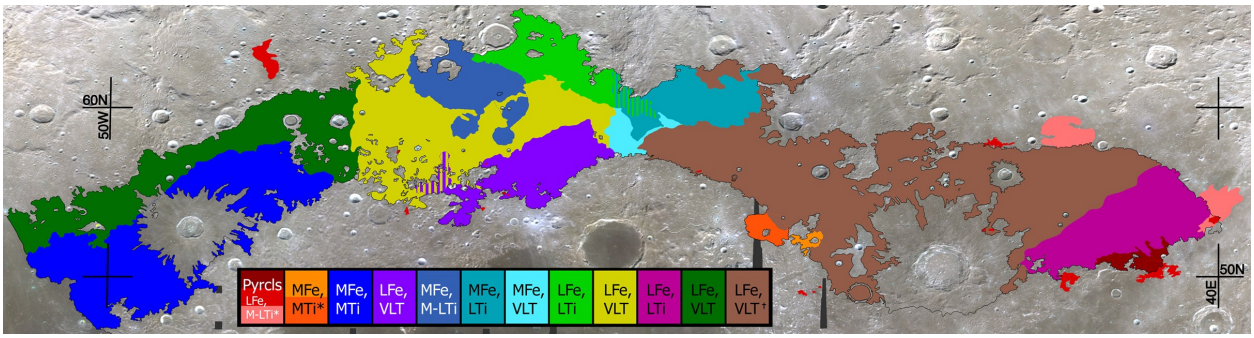

Figure 1: Mare basalt units of Frigoris. Base image is Clementine false color (R=900 nm, G=750 nm, B=415 nm). Abbreviations: Pyrcls=Pyroclastic materials, Fe=Ferric iron abundance, Ti=Titanium dioxide abundance, L=Low, M=Mid, VLT=Very Low Ti. *Interpretation based on surface spectra only (not SCREP). †Aristoteles ejecta and secondaries precluded completion of analysis of this region before abstract submission.

Introduction: Mare Frigoris is an intriguing region for a number of reasons, not least of which is its elongated shape - an atypical feature among its circular-shaped brethren. Orbital photographs and other remote sensing data reveal a diverse geology including stress fractures, gravity anomalies, light plains deposits, volcanic vents, rilles, pyroclastic deposits, cryptomare, and diverse basalt compositions [1-3]. Previous work has recognized and mapped multiple basalt units, the diversity of lithologies, and ages of the units based on surface spectroscopy and crater counting [4]. This work seeks to distinguish the basalt units based on their pristine compositions, that is, as they were when fresh, and independent of subsequent overprinting by large impact craters and gardening by smaller impacts. This is the continuation of our work to map and characterize the pristine basalts in Frigoris, which began with Eastern Mare Frigoris [5].

Data & Methodology: Spectral analysis used 100 m/pixel resolution, 5-band Clementine UVVIS data and 500 m/pixel resolution, 6-band NIR data. To improve analytical efficiency, the NIR data was resampled to the UVVIS resolution and the two datasets combined to make one seamless 11-band image cube. FeO abundance and optical maturity (OMAT) maps were created using the methods of [8]. The TiO_2 abundance map was generated using the method of [9].

The initial division of the maria into discrete basalt units used Clementine albedo and spectral parameter maps of the surface. Mare unit boundaries were further refined and new units added based on sub-regolith com- positional information using results from Small Crater Rim and Ejecta Probing [SCREP, 10] (Fig. 1). Characterizing pristine bedrock lithologies is necessary to accurately assess the geology of the Moon. Optical remote sensing instruments cannot penetrate the several meters-thick surface regolith which blankets the bedrock. We use small, immature craters to look through the obscuring regolith [10-13]. Impact cratering studies and analysis of impact ejecta mechanics demonstrate that near the crater rim the original stratigraphy of the impact target is inverted [e.g., 12]. Therefore collecting data from this region provides the best approach to deriving the composition of the underlying basaltic unit [10]. Craters and their ejecta are delineated that are sufficiently large to hinder obtaining a reliable composition of the underlying basalt despite using SCREP.

Selection of fresh craters for analysis (CFAs) is constrained by their maturity and size. We used the OMAT algorithm of [8], which is optimized for mare basalts and ranges from -0.65 (lowest maturity) to -1.05 (highest maturity). The fresher the crater, the least is the amount of post-impact regolith build-up. We constrained the selection of CFAs to those with OMAT values > - 0.995. The size of the craters is constrained to a diameter of 0.5-5 km. The lower limit on the size is dictated by the spatial resolution of the satellite data while the larger craters are neglected due to likely having penetrated the mare unit. The craters are selected so as not to be affected by any nearby (at least two crater radii away) fresh crater. A total of 796 CFAs satisfying these criteria were identified for Mare Frigoris. We extract compositional information from pixels that depict the rims and proximal ejecta of each CFA. These pixels are used to calculate a single, average spectrum (from 415 nm to 2780 nm), maturity, FeO, and TiO_2 abundance for each CFA.

Analysis: Spectra from all CFAs clearly exhibit a mafic absorption at 1 μm (due to the presence of olivine and/or pyroxene). The absorption at 2 μm (due to pyroxene) is not as readily apparent in all CFAs. This

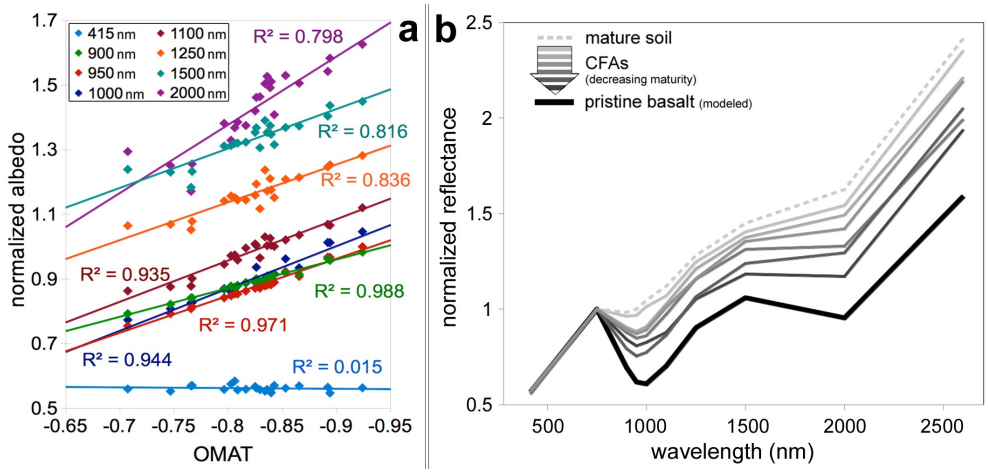

Figure 2: Example of the regression plot (**a**) and normalized spectra (**b**) used to model the pristine basalt spectrum (heavy black line in **b**) representative of a mare unit within Frigoris. The unit shown here is the low-Fe, VLT yellow unit shown in Fig. 1.

is likely an effect of the distortion of the continuum spectra by an increased signal in the longer wavelengths channels (2600 and 2780 nm) due to thermal emission from the surface. These channels were never calibrated in the higher (NIR) wavelength region. Another cause could be more advanced weathering of the surface than indicated by the OMAT parameter. The OMAT parameter is calculated only using channels from the UVVIS camera. Recent studies have shown that the reddening of a soil as it matures does not affect the spectrum uniformly across all wavelengths [15, 16]. changes in the continuum due to space weathering are different in different parts of the spectrum.

It is unlikely that the pristine basalt composition is truly represented in any of the CFAs. Despite focus on fresh craters, regolith production is progressively obscuring the exposed bedrock. Thus, CFAs spectra suffer variations in the albedo of different wavelengths due to contamination from outside terrains as well as spectral weathering. Nonetheless, lower maturity craters are expected to be less contaminated than their more mature brethren, and their spectra closer to that of the pristine basalt. Thus, in the absence of a truly pristine basalt spectrum we hypothesize that we can approximate one if the spectra and OMAT values for the CFAs from a single basalt unit demonstrate a linear trend.

The CFA spectra must be normalized to their 750 nm reflectance to remove albedo variations not associated with composition (e.g., photometry) and focus on the trending behavior of the spectral features associated with mafic composition. We plotted each band's normalized albedos against their OMAT values for all CFAs within a nominally limned mare unit (Fig. 2a). The OMAT parameter and normalized albedos show a good linear relationship for all spectral channels. We used the linear regression to model the pristine basalt spectrum by extrapolating each normalized spectral channel to an OMAT value of -0.6. A fit to the linear trend between the 750 nm albedo (not normalized) and OMAT value was used to calculate the reflectance value used to convert the modeled normalized spectrum to an absolute (modeled) reflectance spectrum.

Results: Although all delineated units have yet to be analyzed, thus far the modeled spectra are good representatives for the pristine basalt in its respective region. This assessment is based on expected characteristics of a fresh basalt spectrum; the continuum slope is low and the depths of the mafic absorptions at both 1 and 2 μm are greater than any of the CFAs within the same unit.

Mare Frigoris is dominated by low-Fe and low-Ti basalt units; the highest FeO and TiO_2 abundance observed in any CFA does not exceed 18 wt% and 6.5 wt %, respectively. In fact, several of Frigoris' basalt units push the lowest bounds for FeO abundances of sampled lunar basalts. Such low FeO concentrations suggests much of Frigoris may be filled with high-Al basalts; a lunar basalt type of interest as a means of better understanding lunar mantle evolution and the lunar magma ocean [e.g., 15]. We will continue to explore Frigoris, and incorporate incorporating data from the Kaguya spectrometers and Moon Mineralogy Mapper to better characterize the basalt compositions and mineralogy.

References: [1] Lucchitta B. K. (1972) *USGS map* I-725. [2] Whitford-Stark J. L. and Fryer R. J. (1975) *Icarus*. [3] Hawke B. R. et al. (2008) *LPS XXXIX*, Abstract #1512. [4] Hiesinger H. et al. (2010) *JGR 115*. [5] Kramer G. Y. et al. (2009) *LPSC XL* Abstract #2369. [6] Wilcox B. B. et al. (2005) *JGR 110*. [7] Lucey P. G. et al. (2000) *JGR 105*. [8] Kramer G. Y. (2010) *Adv. Space Res., 45*. [9] McCord T. B. and Adams J. B. (1973) *Moon 7*. [10] Staid M. I. And Pieters C. M. (2000) *Icarus 145*. [11] Kramer G. Y. (2008) *JGR 113*. [12] Melosh H. J. (1989). *Oxford Univ. Press*. [13] Noble S. K. et al. (2007) *Icarus 192*. [14] Lucey P. G. and Noble S.K. (2008) *Icarus 197*. [15] Neal C. R. and Kramer G. Y (2006) *Am. Mineral. 91*.